MULTIFUNCTION PHASED-ARRAY RADAR: TIME BALANCE SCHEDULER FOR ADAPTIVE WEATHER SENSING

Ricardo Reinoso-Rondinel[1,2,*], Tian-Y. Yu[1,2], and Sebastián Torres[2,3,4]

[1] School of Electrical and Computer Engineering, University of Oklahoma, Norman, Oklahoma, USA
[2] Atmospheric Radar Research Center, University of Oklahoma, Norman, Oklahoma, USA
[3] Cooperative Institute for Mesoscale Meteorological Studies, University of Oklahoma, Norman, Oklahoma, USA
[4] and NOAA/OAR National Severe Storm Laboratory, Norman, Oklahoma, USA

Abstract

Electronically steered phased array radar was developed in mid-1960s mainly for military applications. It has the capability of instantaneously and dynamically controlling beam position on a pulse-to-pulse basis, which allows a single radar to perform multiple functions such as search, target tracking, and weapon controls. The recent-installed phased array radar (PAR) at the National Weather Radar Testbed (NWRT) in Norman, Oklahoma is the first phased array system in the nation dedicated to weather radar research and can electronically steer the beam in both azimuth and elevation. Thus, the PAR has the capability to dynamically adapt its parameters of control in relation to what it senses from the environment of interest. To fully unleash the power of the PAR for adaptive weather sensing, scheduling multiple competitive tasks (i.e. surveillance and storm cells tracking) in a sequence to meet the requirement of the update time for each task is the core of this study.

Time Balance (TB) is an adaptive process that schedules those competing tasks, by balancing the available radar time and the time demanded by each task. In this work, simulated radar data are used to compare the performance of TB-based scanning strategies with the conventional Volume Coverage Pattern (VCP) used in the operational Weather Surveillance Radar- 1988 Doppler (WSR-88D).

1. INTRODUCTION

Continuous technology upgrades on the Weather Surveillance Radar-1988 Doppler (WSR-88D) over two decades have considerably benefited both research and operational communities. The National Weather Service has shown improvement in warning of severe weather after the installation of WSR-88D (Polger et al., 1994). WSR-88D surveils the atmosphere by mechanically rotating the antenna 360°in azimuth at a number of elevation angles. Scanning patterns are known as volume coverage patterns (VCP) and lead to update times from 4 to 6 min for convective storms in order to provide Doppler spectral moments with the required accuracy (ROC, 2007). However, rapid updates are often desirable for understanding fast-evolving weather systems (e.g., Steadham et al., 2002). Although fast update times can be achieved by increasing the antenna rotation rate, the accuracy of spectral moments is usually degraded for the same spatial resolution because fewer samples are available in the dwell time. As a second approach, the research Center for Collaborative Adaptive Sensing of the Atmosphere (CASA) consists of a network of X-band radars that can mechanically scan the regions with rapidly-evolving weather more frequently, while maintaining the surveillance function (Brotzge et al., 2005). Therefore, for a single radar it is advisable to accomplish, fast revisits over region of interest maintaining data accuracy while nonhazardous regions can be covered at smaller revisit rates which are not feasible with conventional radars.

Phased-array radar (PAR) technology was developed in the mid-1960s primarily for military use (Skolnik, 2001). PARs are capable of steering the beam electronically on a pulse-by-pulse basis. This beam agility makes the PAR an ideal platform to perform multiple functions such as surveillance, multitarget tracking, and weapon guidance. For a multifunction radar, all tasks are competing for a finite radar resource. Therefore, it is important to solve this resource management problem; that is, how to allocate radar resources in an optimal way by executing competing tasks in sequence (e.g., Vannicola et al., 1993; Capraro et al., 2006; Haykin, 2006; Gini and Rangaswamy, 2008). One of such scheduling algorithms that is based on the concept of time balance (TB) was developed by Stafford (1990) and applied to PAR. In this paper, the TB scheduling algorithm is extended for weather applications.

* *Corresponding author address:* Ricardo Reinoso-Rondinel, University of Oklahoma, School of Meteorology, 120 David L. Boren Blvd., Rm 5900, Norman, OK 73072-7307; e-mail: rein3@ou.edu

The PAR installed in the National Weather Radar Testbed (NWRT) in Norman, Oklahoma has become available to research communities since September 2003 (Forsyth et al., 2005). The PAR operates at S-band and is able to electronically steer in elevation and azimuth within a 90° sector. Moreover, recent experiments with the NWRT PAR have demonstrated better and precise characterization of fast-evolving weather systems with fast updates than the WSR-88D (Zrnić et al., 2007; Heinselman et al., 2008). Thus, the NWRT PAR is expected to execute both, multiple weather tracking and a volumetric surveillance to collect data of interest and detect new weather developments, respectively.

In this work, two radar functions, storm tracking and weather surveillance, are of interest to perform adaptive sensing. Two quality measures are defined in section 2 to quantify the trade-offs for such adaptive scanning strategies. In section 3, an algorithm based on TB is introduced to schedule competing surveillance and storm tracking tasks for weather sensing. To demonstrate the performance of TB scheduling and its impact on the two quality measures, simulations based on interpolation of real data to a finer time scale are conducted in section 4. Finally, a summary and conclusion are given in section 5.

2. QUALITY MEASURES FOR ADAPTIVE WEATHER SENSING

Conventional radars that use mechanical scanning (e.g., the WSR-88D) typically scan a volumetric region with update times of 4 to 5 min. As a result, the update time for each storm cell is the same and equal to the revisit time of the volumetric region. On the other hand, a PAR system is flexible enough so that it can revisit multiple storms at different rates to better capture the evolution of weather phenomena of interest.

In this work, two radar functions are considered: storm tracking and surveillance. These compete for radar time and need to be properly scheduled. For storm tracking, it is assumed that the information about the size and location of each storm to be scanned is known (e.g., from a storm tracking algorithm). Tracking of each storm cell is defined as a tracking task with its own update time. In contrast, the purpose of the surveillance (herein referred to as the surveillance task), is to scan the volumetric regions where no storms are identified to ensure the detection of newly developing phenomena. Ideally, to fully use the radar resource, surveillance takes place whenever the radar is idle.

For the purpose of scheduling, each tracking task is defined by its task time (T) and update time (U). The task time is the total time needed to volumetrically scan the identified storm. The update time, however, may be set based on users needs. For each task, the occupancy (O) is defined as the ratio of task time and update time (TU^{-1}) (Manners, 1990). The total occupancy is constrained as follows:

$$O_T + O_S = \sum_{i=1}^{N} O_i + O_S = 100\%, \qquad (1)$$

where N is the number of storm cells, O_T is the total tracking task occupancy, $O_i = T_i {U_i}^{-1}$ is the occupancy for the ith task tracking, and O_S is the surveillance task occupancy (Sabatini and Tarantino, 1994). The task time for the surveillance (T_S) is the total time to scan nonstorm regions and the update time for surveillance (U_S) comes from $O_S = T_S {U_S}^{-1}$. If O_T is more than 100%, the radar is referred to as being overloaded.

2.1. Quality measures

For a nonoverload situation, two quality measures are introduced to quantify the performance improvement achieved with adaptive sensing using tracking and surveillance tasks vs. conventional, nonadaptive scanning. The data accuracy for the storm tracking function is set to be equal to that with conventional scanning. However, the data accuracy for the surveillance function is relaxed. The two quality measures are defined and discussed next.

1) Revisit improvement factor

The update time for all storms using WSR-88D scan is the same and denoted by U_C. In this work, U_C is assumed to be the time for completing a full scan over a 90° sector in order to match the electronic scanning limitations of stationary single antenna PAR. The total revisit improvement factor, I, for N tracking tasks is defined by the ratio of the total number of revisits for N storms using adaptive scanning over conventional scanning during a period of time U_m. Matemathically:

$$I = \frac{\sum_{i=1}^{N} U_m {U_i}^{-1}}{N U_m {U_C}^{-1}}. \qquad (2)$$

For N tracking tasks, equation (2) quantifies the gain in the number of revisits yielded by adaptive weather

sensing. Thus, a large I indicates that storms are being revisited more frequently compared to conventional scanning while maintaing the same data accuracy.

2) Acquisition time

A parameter that indicates how long the radar takes to execute all tasks is critical in the context of adaptive sensing. In this work, acquisition time (A) is defined as the minimum time needed to execute each task at least once. Writing equation (1) in terms of task times and update times, and letting U_k be the maximum of U_i for $i = 1, 2, ..., N$; acquisition time can be derived for two conditions as follows:

$$T_k + \sum_{i=1,\neq k}^{N} U_k {U_i}^{-1} T_i + U_k {U_S}^{-1} T_S = U_k, U_k > U_S \quad (3)$$

$$\sum_{i=1}^{N} U_S {U_i}^{-1} T_i + T_S = U_S, U_k < U_S, \quad (4)$$

The ratio of $U_k {U_i}^{-1}$ and $U_k {U_S}^{-1}$ in equation (3) are larger or equal to 1, which means task i can be executed more than once within U_k. In equation (4), when U_k is smaller than U_S, each tracking task is executed at least once while surveillance task is executed only once. As a result, the acquisition time, A, is obtained as:

$$A = max\{U_k, U_S\}. \quad (5)$$

In other words, the task with the longest update time determines the acquisition time.

3. TIME BALANCE SCHEDULING ALGORITHM

A detailed analysis of TB scheduling for tracking multiple point targets was provided in Butler (1998). In this work, TB scheduling is extended to adaptive weather sensing using PAR, that is, the tracking of storm cells. The algorithm associates a time balance variable (T_B) with each tracking task, where a positive time balance indicates the task is late for execution at any given time. Surveillance is only executed when the time balances of all tracking tasks are negative. Therefore, there is no time balance variable associated with the surveillance task. In addition, the surveillance task is executed in fragments. The time needed to dwell on a fragment region is defined as task fragment time (T_F). Only after all fragments are scheduled, the surveillance task is said to be completed.

A flow chart of the TB scheduling algorithm for weather sensing is presented in Figure 1. The first step is to acquire information about the storms from the tracking algorithm. This information consists of the number of storm cells, their location and size, and their required update times. The fragment time for the surveillance task can also be user defined. The second step is to set the time balance variable of any new tracking tasks to zero. The third step is to evaluate the time balance of all the tracking tasks. If one of the tracking tasks has nonnegative T_B, step 4 will be reached, where the task with the maximum T_B (e.g., task i) will be selected. In step 5, the T_B of task i, ${T_B}^{(i)}$, will be decreased by its update time (U_i), while the T_B for the rest of the tasks are maintained. In step 6, task i is scheduled. On the other hand, if in step 3 the time balance of all tracking tasks are negative, indicating that all tasks are on time, a fragment of surveillance is then scheduled. Moreover, the T_B of each task is increased by the task time (or fragment time in the case of surveillance) of the scheduled task when this task is completed. This procedure is repeated until no more tasks are to be scheduled. The general idea of the TB algorithm is to schedule each task as it was originally requested. Therefore, the TB algorithm schedules these competing tasks by balancing the available radar time and the requested update time of each tracking task.

4. SIMULATION RESULTS

Data observed by the WSR-88D is used to simulate PAR observations. In this section, a case of multicell storms observed by the WSR-88D in Twin Lakes, Oklahoma (KTLX) on 22 April 2008 is used to demonstrate the TB scheduling for adaptive weather sensing with the goal of providing fast update time for storms without comprising data quality. Over a period of 100 minutes, a single storm cell split into two cells at approximately 0125 UTC and later the one on the north side further split and three cells were observed by the radar. Reflectivity from selected times at elevation of 0.5°is shown in Figure 2. The KTLX data was linearly interpolated in time at each elevation to reproduce a more frequent weather data set every 15 s. In this way we can simulate the process of TB scheduling with the NWRT PAR. In this work, the storm cells are identified based on some of the concepts used in the storm cell identification and tracking algorithm (SCIT) (Johnston et al., 1998), but in a simpler manner. Figure 2 shows a 35 dBZ contour for each identified cell and their azimuthal extent limited by red, blue, and cyan lines for cells 1, 2, and 3, respectively.

For the tracking tasks, the task time is the time needed to complete the volumetric scan of the identified storm in using the same dwell times as in the WSR-88D VCP.

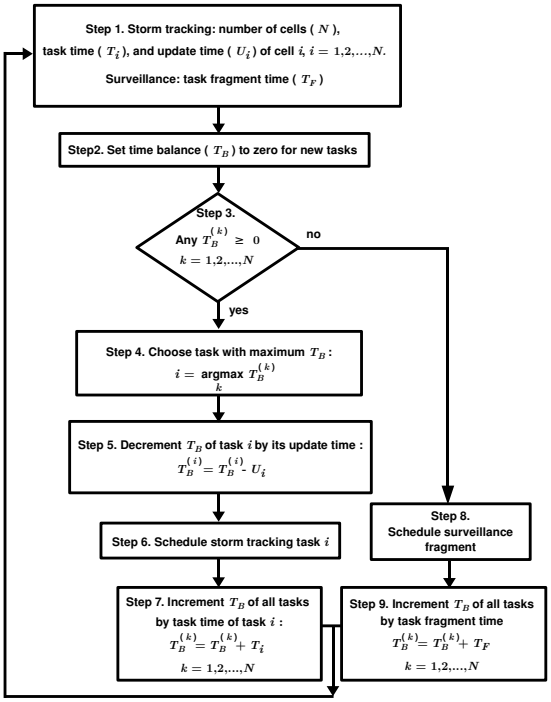

Figure 1: Time Balance scheduler algorithm flow chart. The scheduler algorithm selects tracking task with maximum nonnegative T_B for the next tracking task execution (left branch). Otherwise, surveillance is scheduled (right branch). T_B for each tracking task is updated on every iteration.

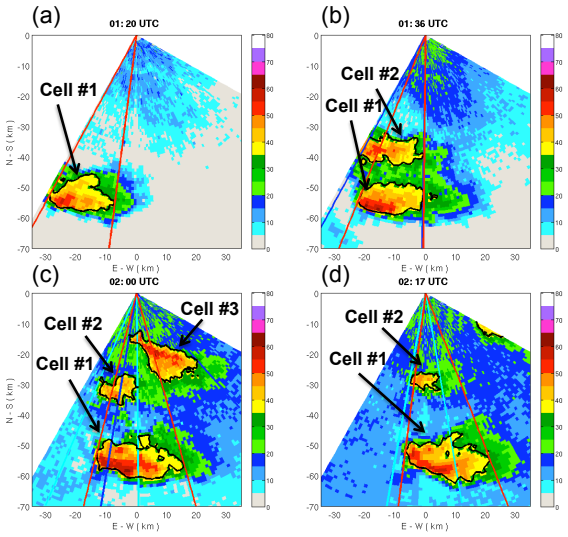

Figure 2: Reflectivity data of storm cells at 0.5°elevation angle in Central Oklahoma on 22 April 2008. (a) cell 1 bounded by a contour of 35 dBZ. (b) cell 2 moving north, split from cell 1. (c) cell 3 moving east, split from cell 2. (d) shows cell 3 has left 90°sector.

Note that tracking tasks cannot be interrupted by other tasks. For the surveillance task, the dwell time is fixed for all elevations at 9.2 ms. This is the same as the shortest dwell times used for detection in VCP 12 (i.e., long-PRT pulses of Batch mode). Surveil task fragments are determined by grouping beam positions by elevation angles. Then, T_S is the sum of T_F over all the elevations in the scanning strategies. To facilitate discussion, the entire simulation interval from 0120 to 0300 UTC is divided into three periods based on the number and size of storm cells. Period 1 (0120-0140 UTC) contains cell 1 only, and then cells 1 and 2. Period 2 (0140-0215 UTC) contains cells 1, 2, and 3. Period 3 (0215-0300 UTC) contains both cells, 1 and 2, and then only cell 1. Requested update times are set as follows. For period 1, U_1 is 35 s and after cell 2 appears, U increases to 40 s for both of them. For period 2, U increases to 45 s for all cells. For period 3, U decreases to 30 s. Surveillance task execution does not have an associated T_B; however, its occupancy and resulting update time can be estimated from equation (1).

The performance of the TB scheduler is assessed by comparing the requested and actual executions of tasks. The occupancy, acquisition time, and revisit improvement factor are calculated using a sliding window with size given by the acquisition time. Figure 3 exemplifies nonoverload and overload cases through the TB scheduling obtained from this simulation. Moreover, task times, update times, and occupancies are shown

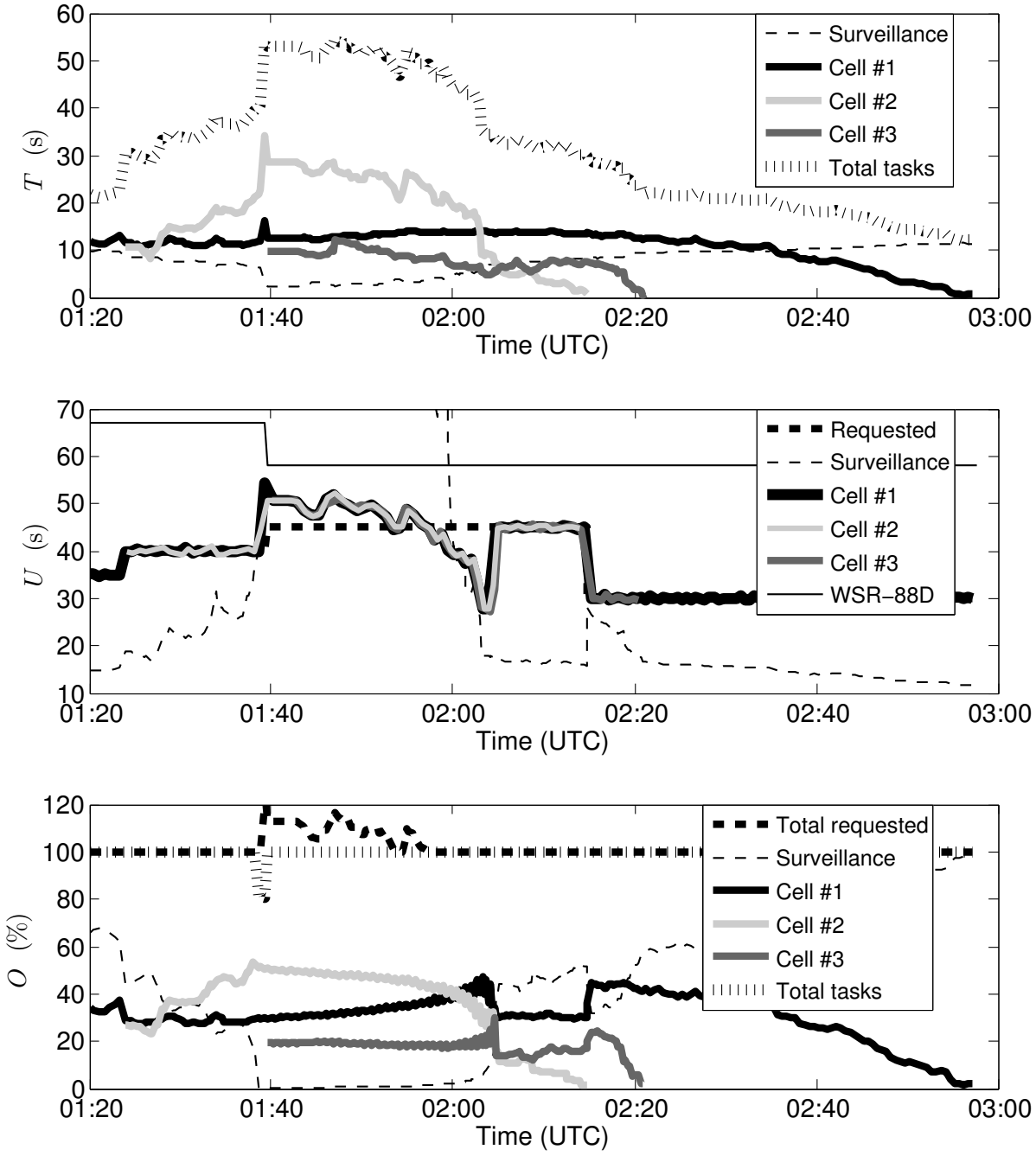

Figure 3: (top) task times for cells 1, 2, 3, and surveillance, black, light gray, gray solid lines, and black dashed thin line, respectively. The sum of task times is represented by black big dotted line. (middle) update times for every storm cell and surveillance. Black dashed thick and thin lines are the requested update time for each cell and surveillance, respectively. Actual update times for cell 1, 2, and 3, are represented by black, light gray, and gray solid thick lines. In addition, U_C is showed by black solid thin line. (bottom) occupancies for each storm cell and surveillance. Total requested and actual occupancies are represented by black dashed thick line, and black big dotted line, respectively.

on top, middle, and bottom panels of Figure 3. Task times for tracking cells 1, 2, and 3 are represented by black, light gray, and gray solid lines on the top panel of Figure 3. In addition, task time for surveillance and the total task time demanded by all tasks are indicated by black dashed thin and black big dotted lines, respectively. Furthermore, for tracking tasks, the requested update time for each period is shown by the black dashed thick line on the middle panel of Figure 3. Update time for the surveillance task is plotted by black dashed thin line. In addition, the update time for a 90°sector of KTLX, U_C, is represented by the black solid thin line. Actual update times obtained from the TB scheduler are graphed in black, light gray, and gray solid thick lines for cells 1, 2, and 3, respectively. For periods 1 and 3, the requested and actual update times for storm tracking tasks agree well. However, for the interval of 0140 to 0155 UTC in period 2, the actual U is larger than the requested one. The reason for tasks being scheduled late is that the requested U of 45 s is smaller than the total task time specified by each task, top panel of Figure 3. Now, within 0155 and 0205 UTC the actual update time becomes smaller than the requested one because storm tracking tasks are executed late and in order to reach a balance, the scheduler forces faster than requested execution of tracking task. Estimated occupancies are shown on the bottom panel of Figure 3. The total requested occupancy is the ratio between T and U and is indicated by the black dashed thick line. As it can be seen, within the interval of 0140 and 0155 UTC the requested total occupancy is higher than 100%; i.e., the scheduler is overloaded. The total actual occupancy is maximized at 100%, which implies no idle time. The actual occupancies of each storm tracking and surveillance task are plotted using the same line style as the two upper panels.

Herein, the envelope of T_B ($\widetilde{T_B}$) is defined as the set of the values of T_B every time a storm tracking task is executed. Thus, $\widetilde{T_B}$ is either zero or positive. $\widetilde{T_B}$ can be used to observe whether a task is executed on time. This is shown on the top panel of Figure 4. The overload period is reflected on the $\widetilde{T_B}$ for the tracking tasks. For the time interval from 0140 to 0155 UTC, every $\widetilde{T_B}$ increased with time. During this interval only tracking tasks were executed; i.e. surveillance is critically delayed. Between 0155 and 0205 UTC, each $\widetilde{T_B}$ decreased with time because tracking tasks were scheduled in time intervals smaller than the requested U. After 0205 UTC, $\widetilde{T_B}$ behaves normally as expected for a nonoverloaded case.

In this simulation, the acquisition time is computed after each scheduling, by counting the minimum time in which all the tasks are executed at least once. Both the theoretical and estimated acquisition times are present in the middle panel of Figure 4. The theoretical A is denoted by the black dashed line and the estimated A by a thin line with asterisks. In addition, the acquisition time for KTLX is indicated by the black solid line. Figure 4 shows that the theoretical and estimated acquisition time agree well except for the period of overload, in which only tracking were scheduled. Note however that the estimated A is always smaller than the acquisition time for KTLX for nonoverload case. This indicates adaptive sensing can complete the requested tasks in a relatively short period of time compared to standard scanning. Finally, the revisit improvement factor can be used to quantify how frequently the storms are scanned compared to the WSR-88D. Theoretical and estimated I are shown on the bottom panel of Figure 4. Also, the line of $I = 1$ means no gain on the number of revisits from the adaptive sensing over conventional scanning. Similarly to the acquisition time, the theoretical and estimated improvement factors are consistent except when overloading occurs. When the overload situation begins, the estimated I shows a constant increment compared to the theoretical I. This is due to the earlier execution of tracking tasks. $\widetilde{T_B}$ shows a "catch up" period to compensate delays on tracking tasks (top panel of Figure 4). During the entire simulation, each storm is revisited more frequently compared to the KTLX standard scan, while the same data accuracy is maintained. In addition, for the cases with no overloading based on the requested update times assigned to each storm tracking task, estimated A and I are within the satisfactory range defined in section 2.

For the cases with no overloading, the results have demonstrated a possible adaptive weather sensing for PAR based on TB where more frequent visits on storms from conventional radars can be provided while maintaining the same data quality. The TB scheduler algorithm is capable of executing tracking tasks satisfying requested update times or occupancies.

5. SUMMARY AND CONCLUSIONS

For conventional radars, the trade-off between fast updates and high data quality for weather applications is inexorable. Phased array systems are suitable to overcome such trade-off. In fact, PAR technology may lead to increased warning lead times and better understandings of the dynamics on fast-evolving weather phenomena. PAR are suitable to perform multiple tracking and surveillance tasks in an adaptive sensing paradigm. Therefore, it is important how to allocate radar resources

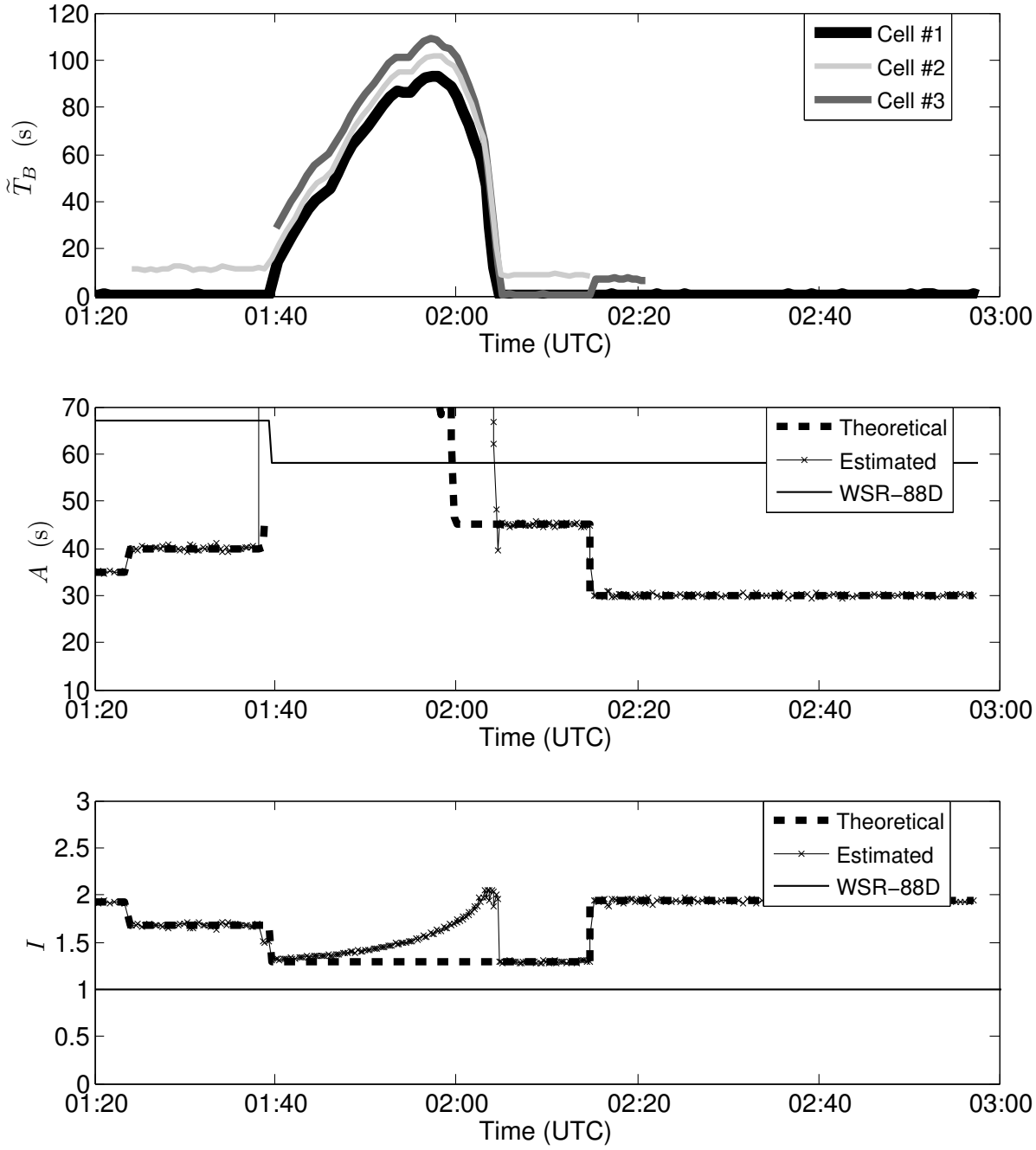

Figure 4: (top) envelop time balance $\widetilde{T}_B$ for cells 1, 2, and 3, black, light gray, and gray lines. (middle) acquisition time A for all tasks. Theoretical and estimated acquisition times are denoted by black dashed line and thin line with asterisks, respectively. In addition, conventional acquisition time is showed by black solid line. (bottom) total revisit improvement factor I. Theoretical, estimated, and conventional revisit improvement factors keep same line styles.

in an optimal way by executing competing tasks in sequence. In this work, a TB scheduler algorithm is presented for this purpose. Two quality measures were introduced: revisit improvement factor and acquisition time. Both measurements were used to evaluate the performance of adaptive sensing relative to that of conventional scanning.

Reflectivity data taken from KTLX was used to test the TB scheduler algorithm for the execution of three storm tracking tasks on the NWRT PAR. Actual update times (occupancies), and estimates of (1) acquisition time and (2) revisit improvement factor were calculated to evaluate such adaptive sensing and assess the performance of the TB algorithm. Simulation showed good agreement between the theoretical and estimated results except in overloading situations. In summary, the TB scheduler algorithm is a vital component in a multifunction PAR system. Such algorithm may prove to be key in balancing the execution of competing radar tasks. It is foreseen that in such adaptive weather sensing context, users of weather products will benefit from better data interpretation leading to significant improvements on weather warnings and forecasts.

ACKNOWLEDGEMENT

This work was primarily supported by NOAA/NSSL under Cooperative Agreement NA17RJ1227. Part of this work was supported by DOD, EPSCoR Grant N00014-06-1-0590.

References

Brotzge, J. A., K. Brewster, B. Johnson, B. Philip, M. Preston, D. Westbrook, and M. Zink, 2005: CASA's first testbed: Integrated project #1 (IP1). in *32nd Conference on Radar Meteorology*, p. 14R.2. AMS.

Butler, J. M., 1998: *Tracking and control in multi-function radar*. Ph.D. thesis, University College London, London, UK.

Capraro, G. T., A. Farina, H. Griffiths, and M. C. Wicks, 2006: Knowledge-based radar signal and data processing. *IEEE Sig. Proc. Mag.*, pp. 18–29.

Forsyth, D. E., J. F. Kimpel, D. S. Zrnic, R. Ferek, J. F. Heimmer, T. McNellis, J. E. Crain, A. M. Shapiro, R. J. Vogt, and W. Benner, 2005: The national weather radar testbed (phased-array) becomes operational. in *21th International Conference on Interactive Information and Processing Systems (IIPS) for Meteorology, Oceanography, and Hydrology*. AMS.

Gini, F., and M. Rangaswamy, 2008: *Knowledge-Based Radar Detection, Tracking, and Classification*. Hoboken, N.J. : Wiley-Interscience, c2008.

Haykin, S., 2006: Cognitive radar. *IEEE Sig. Proc. Mag.*, pp. 30–40.

Heinselman, P. L., D. L. Priegnitz, K. L. Manross, T. M. Smith, and R. W. Adams, 2008: Rapid sampling of severe storms by the national weather radar testbed phased array radar. *Wea. Forecasting*, **23**(808-824).

Johnston, J. T., P. L. MacKeen, A. Witt, E. D. Mitchell, G. J. Stumpf, M. . D. Eilts, and K. W. Thomas, 1998: The storm cell identification and tracking algorithm: an enhanced WSR-88D algorithm. *Wea. Forecasting*, **13**, 263–276.

Manners, D. M., 1990: ART - an adaptive array testbed. *IEE Colloquium PG E15 and E11, Real Time Management of Adaptive Radar Systems*, pp. 6/1 – 6/7.

Polger, P. D., B. S. Goldsmith, and R. C. Bocchierri, 1994: National Weather Service warning performance based on the WSR-88D. *Bull. Amer. Meteor. Soc.*, **75**, 203–214.

ROC, 2007: WSR-88D system specification. WSR-88D Radar Operations Center Rep. OWY55, 164 pp. [Available from NOAA FOIA Office, Public Reference Facility (OFA 56), 1315 East West Hwy. (SSMC3), Room 10730, Silver Spring, MD 20910].

Sabatini, S., and T. Tarantino, 1994: *Multifunction Array Radar, System Design and Analysis*. Artech House.

Skolnik, M. I., 2001: *An Introduction to Radar Systems*. McGraw-Hill.

Stafford, W. K., 1990: Real time control of multifunction electronically scanned adaptive radar. *IEE Colloquium PG E15 and E11, Real Time Management of Adaptive Radar Systems*.

Steadham, R. M., R. A. Brown, and V. T. Wood, 2002: Prospects for faster and denser WSR-88D scanning strategies. in *Interactive Sysmp. on the Advanced Weather Interactive Processing System (AWIPS)*, J89-J91, Orlando, FL. American Metr. Soc.

Vannicola, V. C., L. K. Slaski, and G. J. Genello, 1993: Knowledge-based resource allocation for multifunction radars. *Proc. 1993 SPIE Conference on Signal and Data Processing of Small Targets*, **1954**, 410–425.

Zrnić, D. S., J. F. Kimpel, D. E. Forsyth, A. Shapiro, G. Crain, R. Ferek, J. Heimmer, W. Benner, T. J. McNellis, and R. J. Vogt, 2007: Agile beam phased array radar for weather observations. *Bull. Amer. Meteor. Soc.*, **88**, 1753–1766.